Sustainable Chemical Engineering
http://ojs.wiserpub.com/index.php/SCE/

UNIVERSAL WISER PUBLISHER

Research Article

Enhanced Biogas Purification Using Low-Cost Adsorption and Absorption Techniques

Anceita Jepleting[1], Doricah Moraa[1], Dorcas Cheptoo[1], Achisa C Mecha[1,2*]

[1]Renewable Energy, Environment, Nanomaterials and Water Research Group, Department of Chemical & Process Engineering, Moi University, Kenya
[2]Department of Environmental Science, University of Arizona, Tucson, AZ 85721, USA
E-mail: achemeng08@gmail.com

Received: 30 July 2024; **Revised:** 12 September 2024; **Accepted:** 13 September 2024

Abstract: The effectiveness of biogas as a source of energy is hampered by low calorific value and equipment degradation due to corrosive impurities in raw biogas. Current purification techniques are tailored for large scale applications; they use a lot of energy, which are expensive and require high operating skills. In this study, adsorption and absorption at ambient conditions were explored for the removal of CO_2 and H_2S from biogas using NaOH and $Ca(OH)_2$. Activated carbon (AC) from coconut shells and iron oxide from waste iron fillings were used as adsorbents. These waste-derived adsorbents are more affordable and easily accessible, in addition, their use contributes to effective waste management. The effect of biogas concentration, absorbent concentration, and adsorbent mass was evaluated. Synergistic effect of adsorption and absorption; recovery, regeneration and reuse of the adsorbents were assessed. The adsorption capacity was 125.5 mg CO_2/g AC and 58.2 ppm H_2S/g iron oxide. The combined systems attained CO_2 and H_2S removal efficiencies of 98% and 100%, respectively using iron oxide-NaOH; and >95% and 100%, respectively for AC-iron oxide combination. The spent adsorbents were regenerated and reused at least twice. The CO_2 adsorption was best described by the Yoon-Nelson model throughout the entire breakthrough profile with an R^2 value of 0.98 using AC. The low-cost sorbents used have great potential for biogas purification for small scale systems.

***Keywords*:** absorption, adsorption, activated carbon, biogas, fixed-bed, iron oxide

1. Introduction

Biogas is produced by anaerobic digestion of biomass. The composition of biogas depends on the type of feedstock being digested.[1,2] For instance, biogas generated from agricultural waste such as manure comprises 55-65% methane (CH_4) and 35-45% carbon dioxide (CO_2), with traces of hydrogen sulfide (H_2S) and ammonia (NH_3). Biogas produced from food waste has a higher methane content of about 60-70%, due to the high organic content of the feedstock, with CO_2 levels of 30-40%.[3] In contrast, biogas derived from municipal solid waste (MSW) has variable composition influenced by the diverse materials in the waste stream, often 50-60% methane and 40-50% carbon dioxide.[4] Depending on the treatment method, biogas from sewage sludge typically contains different amounts of hydrogen sulfide along with 60-65% methane and 35-40% carbon dioxide. Every type of feedstock has an impact on the composition of biogas, which impacts its usefulness for various applications.[4]

DOI: https://doi.org/10.37256/sce.5220245307

Raw biogas must be purified to obtain pure methane with high calorific value for use as fuel. Currently, large scale biogas purification is achieved using absorption, pressure swing adsorption, and membrane separation among others.[5] Physical absorption using water scrubbing and chemical absorption using amine scrubbing and inorganic solvent scrubbing are employed. High bio-methane recovery of above 97% can be achieved.[6] However, they also have high energy requirements, selective with the chemicals are used, and may corrode the equipment and pose a negative impact on the environment. Membrane separation relies on the selective permeability of membranes to separate biogas components. The technology is very effective for the removal of CO_2, H_2S and moisture. However, membranes are costly and fragile to handle, hence, require good skills to handle.[6] Pressure swing adsorption separates different biogas components based on their molecular characteristics and the affinity of the adsorbent material. High bio-methane recovery (95-99%) can be achieved.[6] However, it requires high investment and operating costs, and extensive process control which makes it unsuitable for small scale applications.

To address the challenges arising from large scale systems, there is a need to develop low cost and easy to use technologies employing locally available materials for biogas purification targeting small scale systems. Typical examples of such systems have employed calcined eggshells for CO_2 removal,[7] wood ash for CO_2 removal,[8] soda ash for H_2S removal,[9] red rock for H_2S removal,[10] iron rich red soils as biogas desulphurization adsorbents,[11] biomass ash to eliminate sulfur, aromatic and halogenated volatile organic chlorinated compounds as well as siloxanes and carbon dioxide from biogas and landfill gas,[1] among others. Compared to zeolite, which costs $5 per kilogram, these sorbents are considered low-cost because they are naturally occurring waste products. Waste items that are readily available locally and are typically disposed of include iron fillings, eggshells, wood ash, soda ash, and biomass ash. Red soils rich in iron and red rock are other naturally occurring resources that are easily accessible and inexpensive to acquire.

To explore synergistic effects, there is a move towards the use of combined absorption and adsorption systems. A combination of local potash for CO_2 and moisture removal and activated charcoal for H_2S removal achieved a decrease in H_2S from 0.57% to 0.02%, CO_2 from 31% to 18% and moisture from 0.93% to 0%.[12] Another study used calcium oxide solution, activated carbon, and Na_2SO_4 resulting in over 95% methane enrichment.[13] A combination involving iron oxide, dry lime and potassium hydroxide achieved a removal efficiency of 86.6% for H_2S and 90% for CO_2.[14] The use of steel wool for H_2S removal, water scrubbing for CO_2 removal and silica gel for moisture removal increased methane concentration from 68% to 90%.[15] Similarly, an H_2S removal efficiency of 96.84% was achieved using monoethanolamide, NaOH, $Ca(OH)_2$, granular activated carbon and steel wool in a packed column.[16] Fixed bed adsorption using steel wool oxidized under atmospheric conditions achieved an H_2S removal efficiency of 95%.[17] Activated carbons have shown improved H_2S removal capacities, particularly when doped with metals or treated with functional groups.[18] To increase overall biogas quality and economic viability, the most recent research highlights the significance of improving adsorbent regeneration procedures and integrating these materials into effective, scalable purification systems.[19]

Based on the promising results from previous studies, the current study developed a biogas purification system using locally available and low-cost materials for small scale level users. Sodium hydroxide, calcium oxide, and activated carbon from coconut shells were used for CO_2 removal. Iron oxide from waste iron chips was used for H_2S removal. Combinations of these materials were also employed, and synergy was determined. The data were fitted to existing fixed bed adsorption models, namely, Yoon-Nelson and Adams-Bohart models. Recovery, regeneration, and reuse of the materials was undertaken to explore long term performance.

2. Materials and methods

2.1 *Materials*

Iron chips were obtained from the lathe machine in the Mechanical and Production Engineering Workshop in Moi University. Coconut shells were obtained as waste in an open-air market in Mombasa County in Kenya. Raw biogas storage bags were sourced from Biogas International Company. The purified biogas sampling bags were obtained from Geotech (China). Sodium chloride, silica gel, hydrogen peroxide, hydrochloric acid (30%), iron sulphide, calcium oxide, sodium hydroxide was obtained from Indo Kenya Enterprises, Eldoret. All the chemicals used in this study were of analytical grade. All solutions were prepared using distilled water.

2.2 *Characterization of raw biogas*

Raw biogas was obtained from two sources: Moi University Farm (sample 1) and Kesses Farm, Eldoret (sample 2). Both raw biogas samples were produced using cow dung as substrate. Their composition was analyzed using a gas analyzer Model: SKY2000-M4 (Shenzhen, China) and the results are shown in Table 1. The hydrogen sulphide content in the biogas was low and therefore it was synthesised in the laboratory by reacting 11 g of iron sulphide with 75 ml of 30% hydrochloric acid solution. The synthesized hydrogen sulphide gas was then spiked to the raw biogas sample 2.

Table 1. Composition of raw biogas

Biogas sample	Methane (%)	Carbon dioxide (%)	Hydrogen sulphide (ppm)
Sample 1	55.45	38.57	
Sample 2	49.43	42.01	428[a]

[a] Spiked

2.3 *Preparation of adsorbents*

2.3.1 *Activated carbon*

Coconut shells were sourced from the local market, cleaned with deionized water and air dried. They were carbonized at an activation temperature of 600 °C for a period of 120 minutes in a muffle furnace (model ELF11/14B 220-240 V 1 PH + N). During the carbonization process, purified nitrogen (99.99%) was passed through at a flow rate of 0.15 L/min. This step of conditioning was necessary to increase the adsorption capacity of the ash. Conditioning leads to the maturation of bottom ash, hardens it and improves its capacity to eliminate H_2S.[20] The product was mixed with 1 L of 6 M aqueous sodium hydroxide solution in a conical flask for activation. After 24 hours, the activated carbon was filtered from the chemical solution, washed with distilled water, and then dried in an oven (model LDO-150), at 120 °C for 6 hours. The dried activated carbon was then crushed using a ball mill before use.

2.3.2 *Iron oxide*

Iron chips (250 g) were sourced from the lathe machine at the Mechanical Engineering workshop at Moi University. They were mixed with 10 g sodium chloride and 50 ml hydrogen peroxide in a sealed container for 10 min.[14] Thereafter, the rusted iron chips (iron oxide) were dried in an oven (model LDO-150), at 100 °C for 2 hours before use.

2.4 *Characterization of activated carbon and iron oxide*

Particle size analysis was done using a Microtrac Sync particle size analyzer. X-ray fluorescence (XRF) analysis was done using Bruker CTX 600 to determine the concentrations of inorganic elements present in the activated carbon. The absorption spectra were analyzed, and concentrations of the elements present in the samples were obtained. X-ray diffraction (XRD) analysis was done using Thermo Scientific ARL Equinox 100 (Generator: 50 W (50 kV/1 mA-Option 30 kV limitation), Micro-focus X-ray tube (Cu, Co, Ag, Mo); Curved Position Sensitive X-ray Detector, CPS 180. Curvature radius: 180 mm, Acquisition in real time over 110° 2 Theta) to study the presence of crystalline structure in the activated carbon.

2.5 *Experimental set-up and process description*

Absorption using $Ca(OH)_2$, NaOH and adsorption using activated carbon and iron oxide were undertaken at ambient temperature.

2.5.1 *Absorption studies*

Experiments were carried out in a transparent plastic container (1 L) tightly corked and fitted with PVC gas inlet and outlet tubes. The container was equipped with a magnetic stirrer to ensure proper mixing of the reacting mixture. The gas inlet tube was connected to a raw biogas collection bag and the outlet tube was connected to a filter and then to a gas sampling bag. Prior to gas sampling for detection, nitrogen (99.99%) was bubbled through the system to avoid oxygen contamination. The effect of absorbent concentration (0.1 M-0.5 M) was investigated at a biogas flow rate of 0.1 L/min. Samples were collected at regular time intervals of 10 minutes to 30 minutes and their composition analyzed using a gas analyzer. Experiments were done in triplicate and average values were recorded.

2.5.2 *Adsorption studies*

The fixed bed adsorption setup consisted of an acrylic plastic column with an internal diameter of 2.1 cm and a height of 30 cm. The adsorbent material was placed in the middle of the column supported by glass wool and glass beads on each end. One end of the adsorption unit was then connected to a raw biogas source and the other end was connected to a filter and then to a gas sampling bag. The system was purged with nitrogen (99.99%) to eliminate oxygen in the system. The effect of adsorbent mass (20-60 g activated carbon and 2-10 g iron oxide) was investigated at a biogas inflow rate of 0.1 L/min. Samples were collected and analyzed as described in section 2.5.1. Experiments were done in triplicate and average values were recorded.

2.5.3 *Combination of sorbent materials*

The combined adsorption-absorption purification set-up is illustrated in Figure 1. It comprised a raw biogas holding tank, a flowmeter, an adsorption unit, an absorption unit, a magnetic stirrer, a filter, a gas sampling bag, and a gas analyzer. Absorption and adsorption units were set up as described in sections 2.5.1 and 2.5.2, respectively. The adsorbents were packed in series in the adsorption unit. Based on preliminary findings, two combinations were applied as follows with adsorption and absorption in series: 10 g iron oxide and 0.5 M sodium hydroxide solution, and 50 g activated carbon and 10 g iron oxide. Experiments were done in triplicate and average values were recorded.

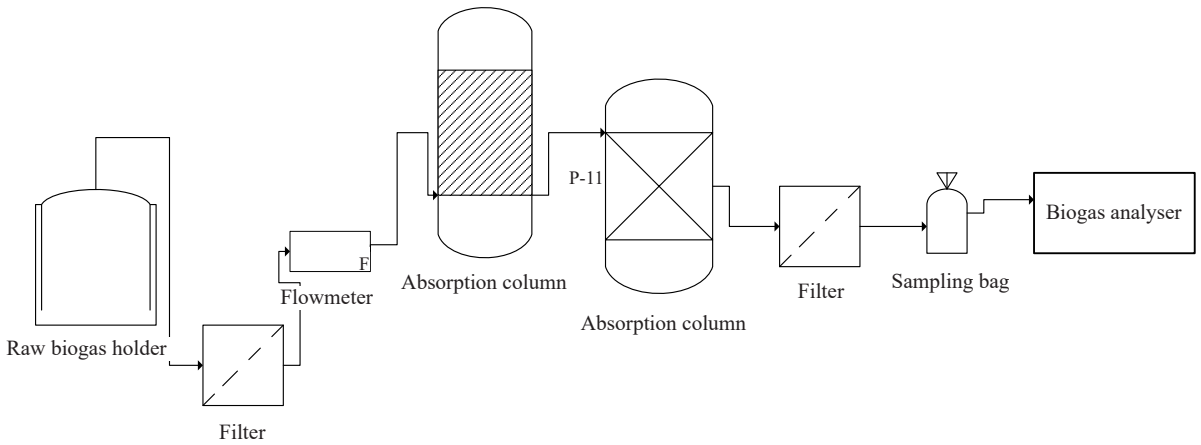

Figure 1. Process flow diagram for the adsorption-absorption purification system

2.6 *Analytical techniques*

The purified and filtered gas was collected in a 1 L multi-layer gas sampling bag with a Polytetrafluoroethylene (PTFE) valve that was sourced from Geotech (China). Biogas concentration (CH_4, CO_2 and H_2S) was measured using a gas analyzer, Model: SKY2000-M4 (Shenzhen, China). Methane enrichment efficiency, CO_2 and H_2S removal

efficiencies were calculated using the following equations based on values in raw biogas and purified biogas:

$$\%CH_4 \text{ enrichment efficiency} = \left[\frac{CH_{4\,\text{purified biogas}} - CH_{4\,\text{raw biogas}}}{CH_{4\,\text{purified biogas}}} \right] \times 100$$

$$\%CO_2 \text{ removal} = \left[1 - \frac{CO_{2\,\text{purified biogas}}}{CO_{2\,\text{raw biogas}}} \right] \times 100$$

$$\%H_2S \text{ removal} = \left[1 - \frac{H_2S_{\text{purified biogas}}}{H_2S_{\text{raw biogas}}} \right] \times 100$$

Fixed bed adsorption models such as Yoon-Nelson model and Adams-Bohart model were used to estimate adsorption capacity of adsorbents.[7]

$$\text{Yoon-Nelson model: } \ln\left(\frac{C_t}{C_o - C_t}\right) = K_{YN}t - \tau K_{YN}$$

Where K_{YN} is the rate constant (per minute) and τ is the time required for 50% adsorbate breakthrough (min). The approach involves a plot of $\ln\left(\frac{C_t}{C_o - C_t}\right)$ versus sampling time (t). The parameters K_{YN} and τ can be obtained using the non-linear regressive method.[7]

$$\text{Adams-Bohart model: } \ln\left(\frac{C_t}{C_o}\right) = K_{BA}C_o t - N_O K_{BA}\left(\frac{z}{v_o}\right)$$

Where K_{BA} (L/mg·min) is the Adams-Bohart kinetic constant, C_o (mg/L) is the saturation concentration, C_t (mg/L) is the concentration at time t, z (cm) is the bed depth, N_O (mg/L) is the maximum gas uptake per unit volume of the adsorbent column and v_o (cm/min) is the linear velocity defined as the ratio of volumetric flow rate, (mL/min) to the cross sectional area, (cm^2) of the bed.

A plot of $\ln\left(\frac{C_t}{C_o}\right)$ vs t gives the values for N_O and K_{BA} from the slope and the y-intercept.

The amount of impurity absorbed by the absorbents was calculated as:[21]

$$Q_{c,t} = \sum_{t=0}^{\text{final}} \left(C_o - \frac{(C_t + C_{t+1})}{2} \right) v$$

$Q_{c,\,t}$ is the amount of CO_2 absorbed until the time of t, t is the finite element time, C_o is the initial CO_2 in gas mixture, C_t is the outlet CO_2 concentration at time t and v is the gas flow rate.

Adsorption capacity of the adsorbents was calculated using the formula:[21]

$$\text{Adsorption capacity}\left(\frac{g}{g}\right) = \frac{(C_O - C_F) \times V \times \rho}{W}$$

Where W is the adsorbent weight of the bed (kg), C_O and C_F are adsorbate concentration in the inlet and outlet of the bed, respectively. V and ρ are gas volume (m^3) and density of the adsorbate (kg/m^3), respectively.

2.7 *Material regeneration and re-use*

The activated carbon and iron oxide adsorbents were regenerated and re-used as follows. The exhausted activated carbon was removed from the bed and thermally regenerated in an oven for 1 hour at 250 °C. The spent iron oxide was removed from the bed and exposed to air for 24 h. The regenerated adsorbents were cooled and then reused as described in section 2.5.2. The adsorption- regeneration cycle was repeated twice and their performance in biogas purification was evaluated.

3. Results and discussion

3.1 *Characterization of adsorbents*

3.1.1 *Particle size analysis of activated carbon and iron oxide*

Figure 2 shows the particle size distribution of the activated carbon and iron oxide used in this study. The average particle size of activated carbon was between 300 and 500 µm and that of iron oxide filings was between 150 and 350 µm. This was within the range reported by Kundu and co-workers.[22]

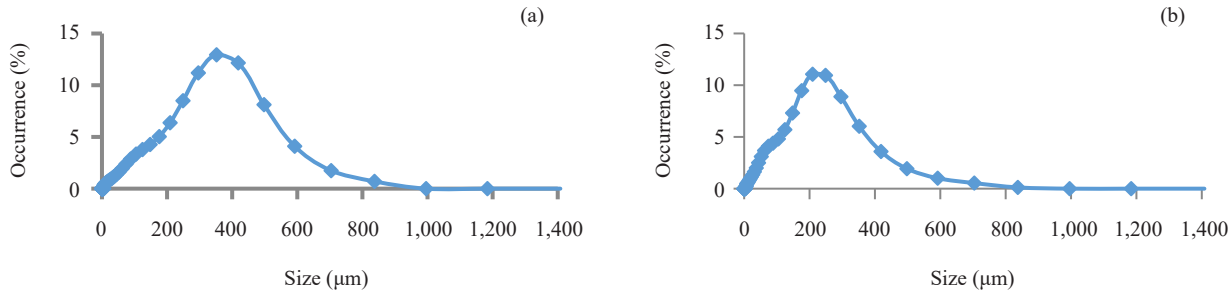

Figure 2. Particle size analysis of activated carbon (a) and iron oxide (b)

3.1.2 *X-ray fluorescence (XRF) analysis of activated carbon and iron oxide*

The chemical composition of the activated carbon according to X-ray fluorescence (XRF) analysis is shown in Table 2. The activated carbon contained a considerable amount of K_2O and Al_2O_3 which important in the adsorption process and this was in agreement with the literature.[23] Iron oxide contained mostly iron as expected and trace amounts of silicon and manganese.

Table 2. X-ray fluorescence (XRF) analysis of activated carbon and iron oxide

Component	Al_2O_3	SiO_2	K_2O	Mn	Fe	Zn
Activated carbon (mg/l)	0.48	0.32	1.12	0.008	0.23	0.002
Iron oxide (mg/l)	0.05	0.8	0.6	0.003	25.5	0.001

3.1.3 *X-ray diffraction (XRD) analysis*

Figure 3 shows the XRD spectra of activated carbon. The appearance of a broad diffraction background and the absence of sharp peaks revealed a predominantly amorphous structure. Two major broad diffraction peaks were observed around 2θ = 24° and 43° corresponding to the diffraction of (0 0 2) and (1 0 0), respectively.[24] This structure makes activated carbon an ideal medium for adsorption.

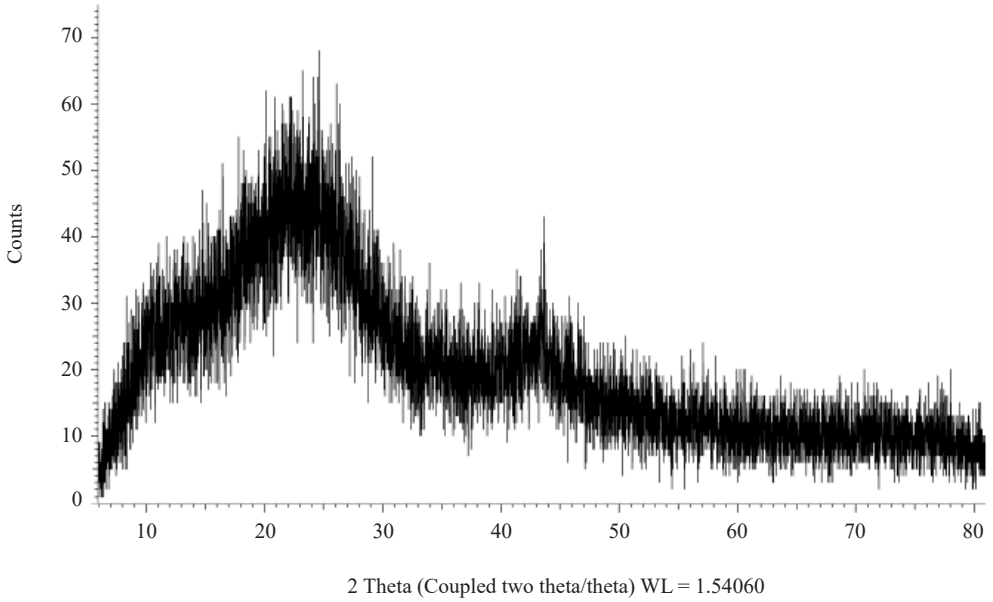

Figure 3. X-ray diffraction (XRD) spectra of activated carbon

3.2 *Biogas purification using absorbents and adsorbents*

3.2.1 *Effect of concentration of $Ca(OH)_2$ solution on CO_2 removal*

The effect of concentration of calcium oxide solution on the removal of carbon dioxide and methane enrichment are shown in Table 3.

Table 3. Methane enrichment and carbon dioxide removal efficiency using $Ca(OH)_2$

Time (min)	CH_4 enrichment (%)			Carbon dioxide removal (%)		
$Ca(OH)_2$ concentration	0.1 M	0.3 M	0.5 M	0.1 M	0.3 M	0.5 M
10	22.5	27.8	28.1	91.0	95.6	99.1
20	19.9	25.1	26.6	89.3	93.7	98.9
30	17.7	22.1	24.4	83.3	91.0	95.9

It was observed that as the concentration of CaO solution increased, there was a corresponding increase in CH_4 enrichment and CO_2 removal. This is because, with increasing concentration, a higher amount of active hydroxide ions is available to diffuse toward the gas-liquid interface and react with CO_2.[25] This leads to an increase in CO_2

absorption rate hence a higher CO_2 removal efficiency and produces an increase in methane enrichment efficiency. The maximum methane enrichment attained was 28.1% with a CO_2 removal efficiency of 99.1%. The performance of the CaO solution was reduced with time for all concentrations. This is attributed to the occupation of chemical reaction sites in the absorbent and formation of products. The fresh absorbent has many active sites that get depleted with time due to continued absorption of CO_2 resulting to increase of CO_2 in purified biogas with time thus reducing the removal efficiency. The results reported here are in agreement with the literature.[26] The principle behind the absorption of CO_2 by CaO solution is such that when CaO is dissolved in water, it forms calcium hydroxide according to the reaction:

$$CaO + 2H_2O \rightarrow Ca(OH)_2$$

Calcium hydroxide formed reacts with carbon dioxide according to the chemical reaction:

$$Ca(OH)_2 + CO_2 \rightarrow CaCO_3 + H_2O$$

The ionic reaction can be represented as:

$$2OH^- + CO_2 \rightarrow CO_3^{2-} + H_2O$$

3.2.2 *Effect of NaOH concentration on CO_2 removal*

The effect of concentration of sodium hydroxide solution on the removal of carbon dioxide and methane enrichment are shown in Table 4.

Table 4. Methane enrichment and carbon dioxide removal efficiency using NaOH

Time (min)	CH_4 enrichment (%)			CO_2 removal (%)		
NaOH concentration	0.1 M	0.3 M	0.5 M	0.1 M	0.3 M	0.5 M
10	10.8	23.4	26.3	79.2	91.3	93.7
20	10.4	23.3	26.2	77.9	90.1	93.6
30	9.8	20.2	24.2	76.6	89.6	92.2

It was observed that as the concentration of NaOH increased, there was a corresponding increase in CH_4 enrichment and CO_2 removal. This is because, with increasing in concentration, a higher amount of active hydroxide ions is available to diffuse toward the gas-liquid interface and react with CO_2.[27] This leads to the increase in CO_2 absorption rate hence higher CO_2 removal and methane enrichment efficiencies. The maximum methane enrichment attained was 26.3% with a CO_2 removal efficiency of 93.7%, these occurred at 0.5 M NaOH concentration. The performance of the NaOH solution was reduced with time for all concentrations. This is attributed to the occupation of chemical reaction sites in the absorbent and formation of products. The fresh absorbent has many active sites that get depleted with time due to continued absorption of CO_2 resulting to increase of CO_2 in purified biogas with time thus reducing the removal efficiency. The CO_2 removal efficiency compared achieved is higher than that in the literature. For instance, 66% CO_2 removal was reported with the use of 3 M NaOH.[28] The difference could be due to the different operating conditions employed.

NaOH reacts with carbon dioxide as follows:

$$2NaOH + CO_2 \rightarrow Na_2CO_3 + H_2O$$

The ionic reaction can be represented as:

$$2OH^- + CO_2 \rightarrow CO_3^{2-} + H_2O$$

CO_2 in raw biogas is physically absorbed in NaOH thereby generating aqueous CO_2 that reacts with OH^- to form aqueous HCO_3.

3.2.3 *Effect of adsorbent (activated carbon) mass on CO_2 removal*

The results on the effect of adsorbent mass on CO_2 removal are shown in Table 5.

Table 5. Methane enrichment and carbon dioxide removal efficiency using activated carbon

Time (min)	CH_4 enrichment (%)					CO_2 removal efficiency (%)				
Activation carbon amount	20 g	30 g	40 g	50 g	60 g	20 g	30 g	40 g	50 g	60 g
10	8.0	11.9	15.8	19.3	22.4	55.6	60.5	68.5	77.5	86.9
20	3.0	6.2	9.8	12.6	17.6	31.6	35.3	60.5	66.6	76.3
30	0.3	1.4	3.5	8.2	10.4	0.4	21.6	47.0	56.8	65.7

It was observed that the methane enrichment efficiency increased with an increase in adsorbent mass. The methane enrichment efficiency decreases with time due to saturation of the adsorbent sites with time. The decrease in removal efficiency with time could also be due to desorption and overlapping of the adsorbent sites so that many free sites are not exposed to the gaseous adsorbates. Similarly, the CO_2 removal efficiency increased with an increase in adsorbent mass. The CO_2 removal efficiency also decreased with time as the adsorbent sites got saturated with use. These findings are consistent with the literature.[26,29] The increase in CO_2 removal efficiency with a mass of the adsorbent is due to the presence of more active sites on a higher mass of adsorbent that present a decrease in the competition of the CO_2 ions for the available binding sites of the adsorbent. Increasing the adsorbent mass means increasing the total surface area and the total number of adsorption active sites.[29] Activated carbon is highly porous hence it is effective in the adsorption of CO_2 from a gaseous mixture. The changes in molecular dipoles of CO_2 through bond stretching motion result in some permanent polarity in CO_2 molecules at ordinary temperature and pressure. The CO_2 molecules undergo attraction and adhesion on the high surface area of activated carbon.[26] The rapid adsorption of CO_2 in the beginning is due to the external surface of the adsorbent, followed by a slower internal diffusion process.[30] Over time, the adsorption rate decreased due to the reduction of active sites because the adsorbent pores are being filled with CO_2 molecules till saturation.[31]

3.2.4 *Effect of adsorbent mass (iron oxide) on H_2S removal*

Raw biogas was treated using different masses of iron oxide (2 g, 4 g, 6 g, 8 g, and 10 g) obtained from (i) oxidation of iron chips from the lathe machine, and (ii) commercial iron oxide. The results are showed in Table 6.

Table 6. Hydrogen sulphide removal efficiency using iron oxide

Time (min)	H_2S removal (%) using iron oxide from lathe machine					H_2S removal (%) using commercial iron oxide				
Iron oxide amount	2 g	4 g	6 g	8 g	10 g	2 g	4 g	6 g	8 g	10 g
10	81.8	90.2	95.1	99.1	100	74.8	85.5	90.7	95.8	100
20	81.1	87.4	92.1	97.7	99.5	72.0	81.5	88.6	94.6	99.1
30	79.0	85.8	90.2	96.7	99.1	68.7	78.5	87.2	93.5	97.7

It was observed that the H_2S removal efficiency increases with an increase in adsorbent mass and decreases with time. The decrease in removal efficiency with time could also be due to desorption and overlapping of the adsorbent sites so that many free sites are not exposed to the gaseous adsorbates.[25] The higher the adsorbent mass the greater the removal efficiency due to more active sites available for adsorption of H_2S. The performance of iron oxide from the oxidation of iron fillings from the lathe machine was better than that of commercial iron oxide in all instances. Iron oxide is an effective adsorbent for hydrogen sulfide and complete removal was achieved using 10 g of within 10 min. This performance is better than that reported in the literature, 89%[13] and 86.6%.[14] Iron oxide reacts with the hydrogen sulfide in raw biogas to form insoluble salts of FeS as follows:[32]

$$Fe_2O_3 + 3H_2S \rightarrow Fe_2S_3 + 3H_2O$$

The resulting iron sulfide can be oxidized to enable the formation of elemental sulfur and the regeneration of the iron oxide adsorbent:[33]

$$3O_2 + 2Fe_2S_3 \rightarrow 2Fe_2O_3 + 6S$$

3.2.5 *Evaluation of the performance of a combination of sorbent materials in biogas purification*

3.2.5.1 *A combination of iron oxide and NaOH*

A combination of iron oxide from lathe machine and NaOH was employed and CO_2 and H_2S removal efficiency was determined together with the CH_4 enrichment. Table 7 shows the results.

Table 7. Biogas purification using iron oxide and NaOH

Time (min)	H_2S removal (%)	CO_2 removal (%)	CH_4 enrichment (%)
10	100	99.1	31.2
20	100	97.8	29.1
30	100	96.8	26.0

The combination achieved CH_4 enrichment, H_2S and CO_2 removal efficiencies of 31.2%, 100% and 99.1%, respectively within 10 min. The combination performed better than the two sorbents separately and the major impurities in biogas (CO_2 and H_2S) were reduced to very minimal amounts hence bio-methane produced had little amounts of incombustibles. Previous studies have also shown the effectiveness of combined systems, for instance, a combination of iron oxide, dry lime and potassium hydroxide achieved a removal efficiency of 86.6% for H_2S and 90% for CO_2.[14]

A combination of NaOH, activated carbon and steel wool showed H_2S and CO_2 removal efficiencies of 49.53% and 94.04%, respectively.[16] The performance reported in the current study is higher than that in other studies in the literature.

3.2.5.2 *A combination of iron oxide and activated carbon*

A combination of iron oxide and activated carbon was used and the results are shown in Table 8.

Table 8. Biogas purification using iron oxide and activated carbon

Time (min)	H_2S removal (%)	CO_2 removal (%)	CH_4 enrichment (%)
10	100	97.7	29.0
20	100	84.3	23.8
30	100	56.8	17.7

The CH_4 enrichment, H_2S and CO_2 removal efficiencies attained were 29%, 100% and 97.7%, respectively. The iron oxide effectively adsorbed H_2S and the activated carbon adsorbed CO_2. The performance decreased with time due to saturation of the materials and this is a major limitation of activated carbon.[34] The carbon dioxide uptake of activated carbon was 1.255 g CO_2/g AC at 10 min and reduced to 0.837 g CO_2/g AC in 30 min; this was in agreement with 1.153 g CO_2/g AC reported in the literature.[35] The corresponding H_2S uptake of iron oxide was 58.2 ppm H_2S/g iron oxide at 10 min and slightly reduced to 57.66 ppm H_2S/g iron oxide in 30 min. However, the challenge of fast saturation of activated carbon can be addressed by recovery, regeneration, and reuse of the adsorbents (section 3.3). The findings showed that a combination of low cost materials such as activated carbon and iron oxide from the lathe machine waste can be successfully employed for biogas purification and upgrading.[14,36] Iron oxide does not get saturated so fast hence it is a potential long-term performing adsorbent for biogas desulphurization.

3.3 *Evaluation of regeneration and re-use of the adsorbents*

3.3.1 *Performance of regenerated activated carbon*

Figure 4 shows the results of methane enrichment and the CO_2 removal efficiency using activated carbon after two cycles of regeneration and reuse.

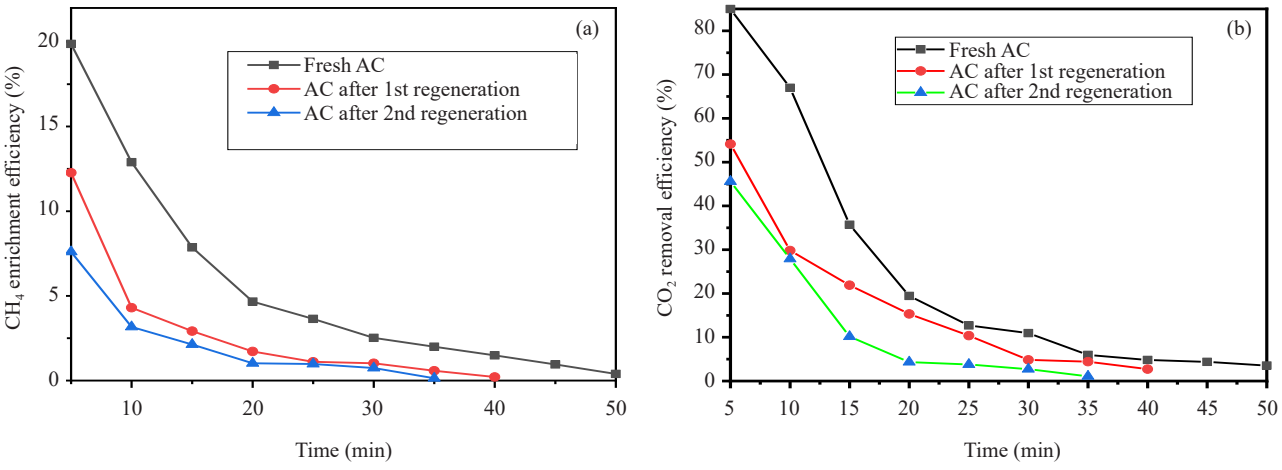

Figure 4. Methane enrichment efficiency (a) and CO_2 removal efficiency (b) with time for fresh and regenerated activated carbon

The activated carbon was regenerated thermally and reused twice. The CH_4 enrichment efficiency and CO_2 removal efficiency were reduced when regenerated activated carbon was used. For instance, at a reaction time of 5 min, the CH_4 enrichment efficiency decreased from 19.88% (fresh AC), to 12.27% (after 1st regeneration) and 7.6% (after 2nd regeneration). Similarly, CO_2 removal efficiency reduced from 84.97% (fresh AC), to 54.13% (after 1st regeneration), to 45.59% (after 2nd regeneration). The regeneration ration was determined by:

$$\text{Regeneration ratio} = \frac{\text{Removal efficiency of regenerated sample}}{\text{Removal efficiencyof fresh sample}}$$

The regeneration ratio was between 0.62 and 0.84 and is the reason why the regenerated AC samples saturated faster compared to the fresh AC. Activated carbon is a very effective adsorbent in gas and liquid cleaning, but its' utility is limited by high purchase cost. Regeneration of spent activated carbon is therefore an economical alternative to save of costs. The regeneration ratio achieved in the present study is higher than that reported in the literature. For instance, one study evaluated the performance of thermally regenerated activated carbon and reported a regeneration ratio of 0.3.[37] Regeneration of activated carbon involves restoring the adsorptive capacity of saturated activated carbon by desorbing adsorbed contaminants on the activated carbon surface.

During thermal regeneration, heat treatment makes the porous structure of activated carbon to be re-exposed and its original surface characteristics are regenerated. Thermal regeneration, however, results in carbon loss of about 5-15 wt.%.[38] In the present study, the 1st regeneration resulted in 6 wt.% carbon loss and 6.8 wt.% carbon loss in the 2nd regeneration. Ashes are also generated during thermal treatment block the pores and resulting in a reduction in the active sites and the adsorption capacity.[38] This could explain why the adsorption capacity of activated carbon reduced gradually after regeneration in this work. The most common regeneration technique employed is thermal regeneration, however, alternative methods include chemical, microbial, and electrochemical regeneration.[39]

3.3.2 *Performance of regenerated iron oxide*

The regenerated iron oxide was used for H_2S removal, and the results are shown in Figure 5.

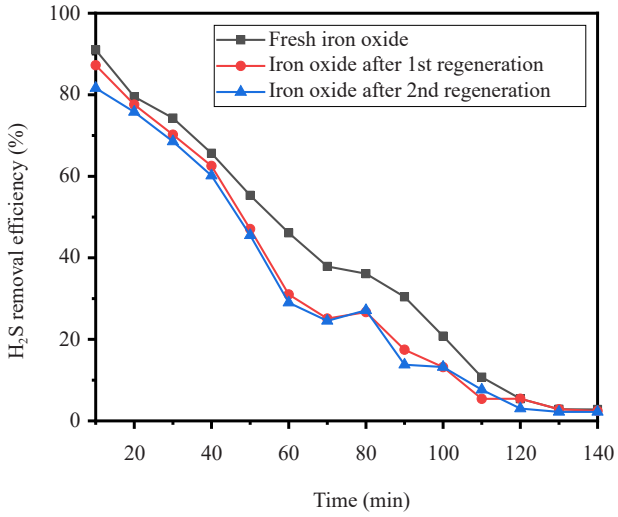

Figure 5. H_2S removal using fresh and regenerated iron oxide

The removal efficiency of H_2S reduced from 91% (fresh) to 87.2% (1st regeneration) and 81.6% (2nd regeneration). Iron oxide adsorbs H_2S from biogas according to equation:

$$Fe_2O_3 + 3H_2S \rightarrow Fe_2S_3 + 3H_2O$$

The H_2S is removed from biogas through the formation of iron sulfide, which is subsequently converted back leaving elemental sulfur on the surface of the porous iron metal chips. The following equation describes the regeneration process. In this process, the pore structure is recovered.

$$2Fe_2S_3 + 3O_2 \rightarrow 2Fe_2O_3 + 6S$$

After regeneration of the saturated iron oxide, there is elemental sulfur remaining due to which the active surface is reduced. This may lead to a reduction in the performance of the regenerated samples as depicted in Figure 5. However, the performance of regenerated iron oxide was comparable to that of the fresh iron oxide. The products formed during the regeneration process are less toxic compared to the hydrogen sulfide. These products can be released to the environment and are used by sulfur-oxidizing bacteria which can be found in freshwater marshes, deep in the ocean, and in the atmosphere.[40] Regeneration of iron oxide entails passing air continuously through the packed bed and some studies have reported doing this for over a week[11] whereas in the present study it was done for 24 h. However, this could depend on other factors such as the amount of iron oxide being regenerated.

3.4 *Application of models to breakthrough profiles of activated carbon*

To predict the fixed bed adsorption performance, the breakthrough data was subjected to Yoon-Nelson and Bohart-Adams models and the parameters are shown in Tables 9 and 10.

The high R^2 vales showed that the Yoon-Nelson model described the experimental breakthrough data appropriately compared to the Adams-Bohart model.

Table 9. Yoon-Nelson model parameters

Bed mass (g)	K_{YN} (min^{-1})	*y*-intercept	τ (min)	R^2
18.64	0.6931	-0.2446	0.3529	0.9513
18.8	0.5095	-0.3569	0.70	0.9759
20	0.5336	-1.3617	2.552	0.8963

Table 10. Adams-Bohart model parameters

Bed mass (g)	Slope	C_o (mg/L)	K_{BA} 10^{-5} (L/mg·min)	*y*-intercept	*Z* (cm)	V_o (cm/min)	N_o (mg/L)	R^2
18.64	0.081	910.8	8.86	-0.479	22.4	7.22	1,742	0.73
18.8	0.089	910.8	9.80	-0.624	22.5	7.22	2,046	0.75
20	0.162	910.8	17.76	-1.302	22.7	7.22	2,563	0.63

4. Conclusions

Evaluation of absorbents (NaOH and $Ca(OH)_2$) and adsorbents (iron oxide and activated carbon) in the removal of CO_2 and H_2S from biogas was done. Adsorbents were successfully prepared and characterized. Activated carbon was prepared from coconut shells and iron oxide from waste iron chips. The effect of absorbent concentration and adsorbent mass on the performance of individual sorbent materials was investigated. The best performance was obtained using a combination of sorbent materials. The combination of NaOH-iron oxide achieved H_2S and CO_2 removal efficiencies of 100% and 99.1% respectively whereas the combination of activated carbon-iron oxide attained H_2S and CO_2 removal efficiencies of 100% and 97.7% respectively. Regeneration and re-use of adsorbents were done. The results showed that the adsorbents can be regenerated and re-used at least twice, a performance that is higher than most works reported in the literature. The Yoon-Nelson model sufficiently described CO_2 adsorption onto activated carbon. The use of activated carbon and iron oxide has great potential for biogas purification. They can be readily regenerated and reused.

Acknowledgement

The authors acknowledge the Africa Centre of Excellence II in Phytochemicals, Textile and Renewable Energy, Moi University for providing financial support.

Conflict of interest

The authors declare that they have no conflicts of interest.

References

[1] Chavez, R.-H.; Guadarrama, J. J. Biogas treatment by ashes from incineration processes. *Clean Technol. Environ. Policy* **2015,** *17*(5), 1291-1300.
[2] Awe, O. W.; Zhao, Y.; Nzihou, A.; Minh, D. P.; Lyczko, N. A review of biogas utilisation, purification and upgrading technologies. *Waste Biomass Valori*. **2017,** *8*(2), 267-283.
[3] Mrosso, R.; Mecha, A. C.; Kiplagat, J. Characterization of kitchen and municipal organic waste for biogas production: Effect of parameters. *Heliyon* **2023,** *9*(5), e16360.
[4] Odejobi, O. J.; Ajala, O. O.; Osuolale, F. N. Review on potential of using agricultural, municipal solid and industrial wastes as substrates for biogas production in Nigeria. *Biomass Convers. Biorefin*. **2024,** *14*(2), 1567-1579.
[5] Niesner, J.; Jecha, D.; Stehlík, P. Biogas upgrading technologies: State of art review in European region. *Chem. Eng. Trans*. **2013,** *35*, 517-522.
[6] Angelidaki, I.; Treu, L.; Tsapekos, P.; Luo, G.; Campanaro, S.; Wenzel, H.; Kougias, P. G. Biogas upgrading and utilization: Current status and perspectives. *Biotechnol. Adv*. **2018,** *36*(2), 452-466.
[7] Mrosso, R.; Mecha, A. C.; Kiplagat, J. Carbon dioxide removal using a novel adsorbent derived from calcined eggshell waste for biogas upgrading. *S. Afr. J. Chem. Eng*. **2024,** *47*, 150-158.
[8] Mulu, E.; M'Arimi, M. M.; Ramkat, R. C.; Mecha, A. C. Potential of wood ash in purification of biogas. *Energy Sustain. Dev*. **2021,** *65*, 45-52.
[9] Mrosso, R.; Mecha, A. C.; Kiplagat, J. Biogas sweetening using new sorbent derived from soda ash from Lake Natron, Tanzania. *Clean. Eng. Technol*. **2023,** *14*, 100646.
[10] Mrosso, R.; Machunda, R.; Pogrebnaya, T. Removal of hydrogen sulfide from biogas using a red rock. *J. Energy* **2020,** *2020*, 2309378.
[11] Pham, C. H.; Saggar, S.; Berben, P.; Palmada, T.; Ross, C. Removing hydrogen sulfide contamination in biogas produced from animal wastes. *J. Environ. Qual*. **2019,** *48*, 32-38.
[12] Orhorhoro, E. K.; Orhorhoro, O. W.; Atumah, E. V. Performance evaluation of design AD system biogas purification filter. *Int. J. Math. Eng. Manag*. **2018,** *3*(1), 17-27.
[13] Mamun, M. R. A.; Torii, S. Enhancement of methane concentration by removing contaminants from biogas

mixtures using combined method of absorption and adsorption. *Int. J. Chem. Eng*. **2017,** *2017*, 1-7.
[14] Shah, D.; Nagarseth, H. Low cost biogas purification system for application of bio CNG as fuel for automobile engines. *IJISET.* **2015,** *2*, 308-312.
[15] Nallamothu, R. B.; Teferra, A.; Rao, B. V. A. Biogas purification, compression and bottling. *GJEDT*. **2013,** *2*(6), 34-38.
[16] Kulkarni, M. B.; Ghanegaonkar, P. M. Hydrogen sulfide removal from biogas using chemical absorption technique in packed column reactors. *GJESM*. **2019,** *5*(2), 155-166.
[17] Magomnang, A.-A. S. M.; Villanueva, E. P. Utilization of the uncoated steel wool for the removal of hydrogen sulfide from biogas. *Int. J. Mech. Eng*. **2015,** *3*(3), 108-111.
[18] Montaño, M. E. A.; Effting, L.; Guedes, C. L. B.; Arizaga, G. G. C.; Giona, R. M.; Cordeiro, P. H. Y.; Tarley, C. R. T.; Bail, A. Performance assessment of activated carbon thermally modified with iron in the desulfurization of biogas in a static batch system supported by headspace gas chromatography. *J. Anal. Sci. Technol*. **2024,** *15*(1), 20.
[19] Coppola, G.; Papurello, D. Biogas cleaning: Activated carbon regeneration for H_2S removal. *Clean Technol*. **2019,** *1*(1), 40-57.
[20] Turgeon, N.; Bihan, Y. L.; Savard, S.; D'aoust, M.; Fournier, M.; Sénéchal, D. Use of municipal solid waste incineration bottom ash for the removal of hydrogen sulphide (H_2S). *Air Pollution XXV* **2017,** *211*, 209-219.
[21] Banisheikholeslami, A.; Qaderi, F. A novel machine learning framework for predicting biogas desulfurization breakthrough curves in a fixed bed adsorption column. *Bioresour. Technol*. **2024,** *25*, 101702.
[22] Kundu, A.; Redzwan, G.; Sahu, J.; Mukherjee, S.; Sen Gupta, B.; Hashim, M. Hexavalent chromium adsorption by a novel activated carbon prepared by microwave activation. *BioResources* **2014,** *9*, 1498-1518.
[23] Aluvihara, S.; Kalpage, C. S.; Bandaranayake, P. W. S. K. Manufacturing of activated carbon using disposable coconut shells. *World News of Natural Sciences* **2020,** *31*, 25-35.
[24] Omri, A.; Benzina, M. Characterization of activated carbon prepared from a new raw lignocellulosic material: Ziziphus spina-christi seeds. *Journal of the Tunisian Chemical Society* **2012,** *14*, 175-183.
[25] Castellanos-Sánchez, J. E.; Aguilar-Aguilar, F. A.; Hernández-Altamirano, R.; Venegas Venegas, J. A.; Raj Aryal, D. Biogas purification processes: review and prospects. *Biofuels* **2024,** *15*(2), 215-227.
[26] Mamun, M. R. A.; Karim, M. R.; Rahman, M. M.; Asiri, A. M.; Torii, S. Methane enrichment of biogas by carbon dioxide fixation with calcium hydroxide and activated carbon. *J. Taiwan Inst. Chem. Eng*. **2016,** *58*, 476-481.
[27] Gallego Fernández, L. M.; Portillo, E.; Borrero, F.; Navarrete, B.; Vilches, L. CO_2 capture for biogas upgrading using salts, hydroxides, and waste. In *Circular Economy Processes for CO_2 Capture and Utilization*; Woodhead Publishing, 2024; pp 7-24.
[28] Maile, O. I.; Muzenda, E.; Tesfagiorgis, H. Chemical absorption of carbon dioxide in biogas purification. *Procedia Manuf*. **2016,** *7*, 639-646.
[29] Sawalha, H.; Maghalseh, M.; Qutaina, J.; Junaidi, K.; Rene, E. R. Removal of hydrogen sulfide from biogas using activated carbon synthesized from different locally available biomass wastes - a case study from Palestine. *Bioeng*. **2020,** *11*(1), 607-618.
[30] Li, W.; Zhang, L.; Peng, J.; Li, N.; Zhang, S.; Guo, S. Tobacco stems as a low cost adsorbent for the removal of Pb(II) from wastewater: Equilibrium and kinetic studies. *Ind. Crop. Prod*. **2008,** *28*(3), 294-302.
[31] Huang, P.-H.; Cheng, H.-H.; Lin, S.-H. Adsorption of carbon dioxide onto activated carbon prepared from coconut shells. *J. Chem*. **2015,** *2015*, 106590.
[32] Ryckebosch, E.; Drouillon, M.; Vervaeren, H. Techniques for transformation of biogas to biomethane. *Biomass and Bioenergy* **2011,** *35*(5), 1633-1645.
[33] Okoro, O. V.; Sun, Z. Desulphurisation of biogas: A systematic qualitative and economic-based quantitative review of alternative strategies. *Chem. Eng*. **2019,** *3*(3), 76.
[34] Vijay, V. K.; Chandra, R.; Subbarao, P. M. V.; Kapdi, S. In *Biogas purification and bottling into CNG cylinders: producing Bio-CNG from biomass for rural automotive applications*, The 2nd Joint International Conference on "Sustainable Energy and Environment (SEE 2006)"; Bangkok, Thailand, 2006.
[35] Durán, I.; Rubiera, F.; Pevida, C. Separation of CO_2 in a solid waste management incineration facility using activated carbon derived from pine sawdust. *Energies* **2017,** *10*(6), 827.
[36] Vivo-Vilches, J. F.; Pérez-Cadenas, A. F.; Maldonado-Hódar, F. J.; Carrasco-Marín, F.; Faria, R. P. V.; Ribeiro, A. M.; Ferreira, A. F. P.; Rodrigues, A. E. Biogas upgrading by selective adsorption onto CO_2 activated carbon from wood pellets. *J. Environ. Chem. Eng*. **2017,** *5*(2), 1386-1393.
[37] Coppola, G.; Papurello, D. Biogas cleaning: Activated carbon regeneration for H_2S removal. *Clean Technologies* **2018,** *1*, 4.

[38] Park, J. E.; Lee, G. B.; Hong, B. U.; Hwang, S. Y. Regeneration of activated carbons spent by waste water treatment using KOH chemical activation. *Appl. Sci*. **2019,** *9*(23), 5132.
[39] Nasruddin, M. N.; Fahmi, M. R.; Abidin, C. Z. A.; Yen, T. S. Regeneration of spent activated carbon from wastewater treatment plant application. *J. Phys. Conf. Ser*. **2018,** *1116*, 032022.
[40] Kuenen, J. G.; Robertson, L. A.; Gemerden, H. V. Microbial interactions among aerobic and anaerobic sulfur-oxidizing bacteria. In *Advances in Microbial Ecology*; K.C., M., Ed.; Springer: Boston, MA, 1985.